View metadata, citation and similar papers at core.ac.uk

brought to you by CORE

provided by Elsevier - Publisher Connector

Available online at www.sciencedirect.com

SCIENCE DIRECT

Developmental Biology 295 (2006) 1 – 12

DEVELOPMENTAL BIOLOGY

www.elsevier.com/locate/ydbio

Mosaic analysis of *extended auricle1* (*eta1*) suggests that a two-way signaling pathway is involved in positioning the blade/sheath boundary in *Zea mays*

Karen S. Osmont [1], Nasim Sadeghian [2], Michael Freeling *

Department of Plant and Microbial Biology, University of California, Berkeley, CA 94720, USA

Received for publication 10 August 2005; revised 26 October 2005; accepted 8 November 2005
Available online 8 May 2006

Abstract

The maize leaf develops in a simple, stereotypical manner; therefore, it serves as a basic model to understand the processes involved in forming developmental boundaries. *extended auricle1* (*eta1*) is a pleiotropic maize mutant that affects proximodistal leaf development. Mutant *eta1* individuals display basipetal displacement of the blade/sheath boundary and the boundary between auricle and blade is not clearly delineated, leading to an undulating auricle. SEM analysis shows that *eta1* is required for proper placement of the blade/sheath boundary on the adaxial leaf surface. Examination of vascular and cellular organization indicates that *eta1* affects not only placement of the blade/sheath boundary, but also differentiation of cell types within the blade/sheath boundary. Genetic mosaic analysis was used to determine the effect of *eta1* mutant tissue on wild-type leaf development and to resolve the site and timing of the *Eta1+* gene product. Interestingly, sectors of *eta1* tissue affect the placement of the blade/sheath boundary even in wild-type tissue. These results suggest that a two-way signaling pathway may be involved in the positioning of the blade/sheath boundary. Based on these data, we propose a model for *Eta1+* function in the maize leaf.
© 2005 Elsevier Inc. All rights reserved.

Keywords: Maize; Leaf development; Mosaic analysis; SEM analysis; Blade/sheath boundary

Introduction

Leaves are determinant lateral organs initiated on the periphery of the shoot apical meristem. In higher plants, leaf initials are specified by negative regulation of class I *knox* (*kn1*-like homeobox) genes by the ARP (ASYMMETRIC LEAVES1/ROUGHSHEATH2/PHANTASTICA) family of Myb-domain proteins (Theodoris et al., 2003; Tsiantis and Hay, 2003). After initiation, leaf primordia adopt their developmental identity and are organized along three main axes: the proximodistal (leaf tip to base), the mediolateral axis (leaf midrib to margin), and the adaxial–abaxial (upper to lower leaf surfaces). Then, cell division and cell expansion give rise to a fully differentiated leaf with distinct domains, containing specific cell and tissue types. While much research has focused on determining the processes by which lateral organs are initiated, the developmental and genetic cues that give rise to different regions (e.g. sheath) or cell types are not as well understood.

Much research in *Arabidopsis*, *Antirrhinum*, and maize has focused on understanding the genetic and molecular processes that give rise to adaxial or abaxial cell fates (Tsiantis and Hay, 2003). For example, members of the *KANADI* and *YABBY* gene families confer abaxial identity, while HD-ZIPIII (class III homeodomain/leucine zipper) genes such as *REVOLUTA*, *PHABULOSA*, and *PHAVOLUTA* ascribe adaxial identity (Hay et al., 2004). However, less is known about how the proximodistal and mediolateral axes are patterned. In maize, the proximodistal axis can be subdivided into three domains: the proximal sheath, the distal blade, and the ligule and auricles, which form the blade/sheath boundary. The ligule is an epidermal fringe of tissue derived from the adaxial leaf surface (Sharman, 1942; Sylvester et al., 1990). The pair of

* Corresponding author.
E-mail address: freeling@nature.berkeley.edu (M. Freeling).
[1] Present address: Plant Gene Expression Center, ARS-USDA, 800 Buchanan Street, Albany, CA 94710, USA.
[2] Present address: University of California, Irvine, College of Medicine, Irvine, CA 92697, USA.

0012-1606/$ - see front matter © 2005 Elsevier Inc. All rights reserved.
doi:10.1016/j.ydbio.2005.11.012

wedge-shaped auricles acts as hinges, allowing the leaf to bend out horizontally from the stem.

Histological studies as well as scanning electron microscopy (SEM) analyses have been used to study early development of the ligule and auricle (Becraft et al., 1990; Sharman, 1942; Sylvester et al., 1990). The first visible sign of ligule region growth is an increase in anticlinal (new walls formed perpendicular to the cell layer) cell divisions on the adaxial epidermis of plastochron 4 primordia, giving rise to the preligule band (Becraft et al., 1990; Sylvester et al., 1990; Walsh et al., 1998). Plastochron (p) is the time interval between leaf initiation events and is a way of measuring the age of a leaf primordium relative to the meristem, with p1 being the most newly initiated leaf. Cells in the preligule band then divide periclinally (new walls formed parallel to the cell layer) in an asynchronous fashion from the midrib to margin to give rise to the ligule ridge (Becraft et al., 1990; Sylvester et al., 1990). Differentiation of the auricles is first visible as a thin line of cells that separate the blade and sheath, and auricle cells are only visible after initiation of the ligule (Becraft et al., 1990). The auricle cells enlarge as the ligule differentiates and then divide as the blade and sheath expand.

Many maize mutants affect proximodistal regional identity, which is manifested by disrupting or displacing development of the blade/sheath boundary. While some previously described maize mutants alter proximodistal regional identity via ectopic expression of *knox* genes, others affect the development of the ligule and auricles. Dominant mutants, such as, *Kn1*, *Gn1*, *Lg3*, *Lg4*, and *Rs1*, ectopically express *knox* genes in the leaves, resulting in the formation of proximal tissues in more distal regions (Becraft and Freeling, 1994; Foster et al., 1999b; Fowler and Freeling, 1996; Smith et al., 1992; Vollbrecht et al., 1991). Two recessive mutants, *liguleless1* (*lg1*) and *liguleless2* (*lg2*), disrupt the blade/sheath boundary by removal of the ligule and/or auricles (Brink, 1933; Emerson, 1912). Genetic and molecular analyses have shown that the *lg1* and *lg2* genes function in the same pathway (Becraft et al., 1990; Harper and Freeling, 1996) and encode a Squamosa-like binding protein (Moreno et al., 1997) and a putative bZIP transcription factor (Walsh et al., 1998). In addition, the dominant mutant *Wavy auricle in blade1* (*Wab1*) was found to interact genetically and molecularly with *lg1* and *lg2*, likely upstream of the *lg* genes (Foster et al., 2004). We identified previously a novel, recessive mutant *extended auricle1* (*eta1*), involved in proximodistal patterning in the maize leaf (Osmont et al., 2003). While double-mutant analysis revealed that *eta1* enhances *Knox* and *lg* mutant phenotypes (Osmont et al., 2003), *eta1* mutant leaves do not display altered expression of genes in these pathway, consistent with action downstream of the *Knox* and *lg* pathways.

To address how *Eta1+* functions in blade/sheath boundary development, we conducted genetic mosaic analyses. Genetic mosaics have been used to help determine the source, target, and meaning of intercellular signals in leaf development. There are two extreme outcomes of a mosaic analysis. Either the mutant phenotype is observed only in the mutant sector, or marked mutant sectors are phenotypically wild-type. For example, when *lg1* mutant sectors are induced in any tissue of a wild-type leaf, that tissue displays a *lg1* mutant phenotype (Becraft et al., 1990), whereas no phenotype is observed when *lg2* mutant sectors interrupt wild-type leaves (Harper and Freeling, 1996). Cell fate within a plant region or organ is largely determined by position (Poethig, 1989). There is evidence, however, that regional identity along the mediolateral axis of the maize leaf is lineage-dependent (Muehlbauer et al., 1997).

Here, we further extend our phenotypic analyses of *eta1* by quantifying the effect on leaf dimensions and by examining vascular and cellular organization of the blade/sheath boundary. We also use SEM analysis to determine when *eta1* mutant defects can first be observed during leaf development. Mosaic analysis reveals that the presence of an *eta1* mutant sector in a wild-type leaf displays an *eta1* phenotype in the sector and affects the development of wild-type tissue on either side of the sector. Based on these data, we suggest that a two-way signaling pathway is involved in positioning the blade/sheath boundary and present a model for *Eta1+* function in the leaf.

Materials and methods

Isolation of the eta1-R allele

The *eta1-R* allele was isolated from an M2 family from an EMS (ethyl–methane sulfonate) mutagenesis performed by the Hollick lab (UC-Berkeley) and was outcrossed for five to six generations to the inbred lines B73, Mo17, W22, and W23 (Osmont et al., 2003). The *eta1-R* allele encodes a monogenic recessive trait and is likely a loss-of-function allele based on the behavior of *eta1* hypoploids (Osmont et al., 2003).

Plant measurements

Measurements were taken of field grown plants in the same family. All measurements were taken at the time of anthesis in *eta1-R* segregating families in the genetic backgrounds W23 and B73. The flag leaf was designated Leaf 17 to guarantee uniform measurements between individuals and between families. Blade length and width and sheath length and width measurements were taken from the 8th leaf to the 17th leaf in order to assay leaves at varying maturities. Blade and sheath widths were measured for half the leaf from midrib to margin and were taken 4 cm above or below the ligule fringe. The leaf measurement data were averaged from nine *eta1* individuals and nine wild-type individuals in both the W23 and B73 backgrounds. Standard deviation was calculated by Microsoft Excel 2000.

Sectioning for fluorescence microscopy

Leaves from an *eta1-R* segregating family in the W23 background were sectioned transversely using a vibratome. Sections of approximately 10–20 cm^2 were cut, mounted, and then sectioned at 80–100 μm. The sections were mounted on coated glass slides in 50% glycerol. The sections were viewed under a Zeiss Axiophot epifluorescence microscope, using a 355–375 nm excitation filter with a 397 nm long pass observation filter. Using these conditions, lignin auto fluorescence is light blue and proto-lignins are bright blue. Images were captured using an Optronics DEI 750 low-light, cooled CCD color video camera and Scion Image J Software. Digital images were processed using Adobe Photoshop 7.0.

SEM analysis

Leaves from 3-week-old seedlings in an *eta1-R* segregating family were dissected and placed on double-sided tape in order of leaf number. Dental impression media (President light body, Coltène) were used to generate

negative impressions of adaxial leaf surfaces. From these negative impressions, Spurr's Resin (Electron Microscopy Sciences) was used for replicas. The replicas were mounted on stubs with carbon dots and then sputter coated with a 15 nanometer coat of 15–20 Å gold/palladium using a BIO-RAD E5400 Sputter Coater. The samples were then imaged using an Electroscan E3 Environmental Scanning Electron Microscope (ESEM) located at the Electron Microscope Laboratory (UC-Berkeley). Digital images were captured using IAAS (Image acquisition and archiving software) from Electroscan, v 1.01 and processed using Adobe Photoshop 7.0.

Mosaic analysis

The previously described *eta1-R* allele was used in this analysis (Osmont et al., 2003). The *eta1* gene maps to bin 5.04–5 on the long arm of chromosome five in maize. The chlorophyll-deficient mutant, *lemonwhite2* (*lw2*), maps to bin 5.05. *lw2* is approximately 35 map units distal to *eta1*. Therefore, *lw2* was chosen as an appropriate marker for mosaic analysis (Maize Genetics Stock Center, Urbana, Illinois). Heterozygous *lw2* individuals were crossed to homozygous *eta1* individuals to obtain crossover events linking *lw2* and *eta1* on the same chromosome arm. The F1 plants were then self-pollinated. Since *lw2* homozygotes have a light yellow seed phenotype and are seedling lethal, only the dark yellow seeds, half of which were heterozygous for *lw2*, were planted. The F2 individuals homozygous for *eta1* (i.e. exhibiting an *eta1* mutant phenotype) and heterozygous for *lw2* (identified by F3 ears segregating the *lw2* kernel phenotype from self-pollinations of *eta1* mutant plants) were outcrossed to the inbreds W22 and W23. Then seeds from these outcrosses, half that were *eta1 lw2*/++ and half that were *eta1*+/++, were subject to X-ray irradiation. Families heterozygous for the *lw2* marker and homozygous *Eta1*+ were also subject to X-ray irradiation to control for any affects of *lw2* on leaf development.

A total of 4650 seeds were imbibed on 150 mm Petri dishes with filter paper for 48 h prior to irradiation. A Pantax 320 kVp X-ray machine was used at Lawrence Berkeley National Laboratory (Berkeley, CA). The X-rays were filtered through a 0.5 mm Copper filter. The dose rate was 100 rad (1 Gy) per minute for 10 min at room temperature. Samples were rotated during treatment to ensure even irradiation. Irradiated seeds were planted directly into the Gill Tract Field (Albany, California) using a hand planter. Plants were observed 2–3 times weekly over 5 weeks for the appearance of white sectors. Since *eta1* is proximal to *lw2*, the closest suitable cell autonomous marker for the mosaic analysis, loss of the *lw2* marker can occur without uncovering *eta1*. Therefore, we selected only white sectors with an *eta1* phenotype because we could not rule out that any particular white sectors without an *eta1* phenotype occurred due to breakage of the chromosome arm between *lw2* and *eta1*. Control sectors carrying only the *lw2* marker were indistinguishable from wild-type (data not shown).

Plants displaying sectors were marked. The sectored leaf or leaves were removed and taken to the lab for analysis. Measurements were taken of the sector width and mediolateral placement on the leaf. Sectors displaying displacement at the blade/sheath boundary were measured relative to the non-sectored half of the same leaf and were photographed. In some sectored leaves, it was difficult to visualize the sector boundary because of the other chlorophyll-containing layers, thus calculations of sector width were inferred from microscopic data and are noted in the results. The sectored leaves were then sectioned transversely using a vibratome (see above). Sectors were imaged using a Zeiss Axiophot epifluorescence microscope with a BP 556/10 nm excitation filter and a LP 590 nm emission filter and equipped with an Optronics DEI 750 low-light, cooled CCD color video camera. Lignin in the cell walls auto-fluoresces yellow-green and chlorophyll red with this filter set. Digital images were captured using Scion Image J and processed in Adobe Photoshop 7.0. As with all sector analysis using chlorophyll-deficient markers, we did not find sectors with mutant *eta1* epidermis and wild-type internal layers because the abundance of chlorophyll in the mesophyll obscures the few stomatal complexes in the epidermis that lack chlorophyll.

Results

The eta1 phenotype affects the transition from distal blade to proximal sheath and is more severe near the leaf margin

In wild-type maize leaves, the boundaries between sheath, ligule, auricle, and blade are well defined (Fig. 1A). However, in *eta1* mutant leaves, the ligule forms normally over the midrib but is disrupted in the marginal domain of the leaf. The boundary between auricle and blade is not clearly demarcated, seen as white auricle tissue extending up into green blade tissue (Fig. 1B, arrows). The excess of auricle tissue results in an undulating auricle instead of a wild-type wedge-shaped auricle (compare Figs. 1C with D). In addition, there is an increase in spacing between lateral veins in the auricle so that they no longer run parallel to the proximodistal leaf axis (Fig. 1D, arrow). These observations show that the *eta1* phenotype affects the transition from distal blade to proximal sheath and is more severe near the leaf margin.

Since *eta1* alters leaf morphology, we wanted to determine any quantitative effects of *eta1* on leaf dimensions. We examined leaf size in a weakly expressing *eta1* background, B73, and in a strongly expressing background, W23 (Osmont et al., 2003). Sheath length was reduced in *eta1* mutants in both backgrounds, while blade length in the *eta1* mutant blade is

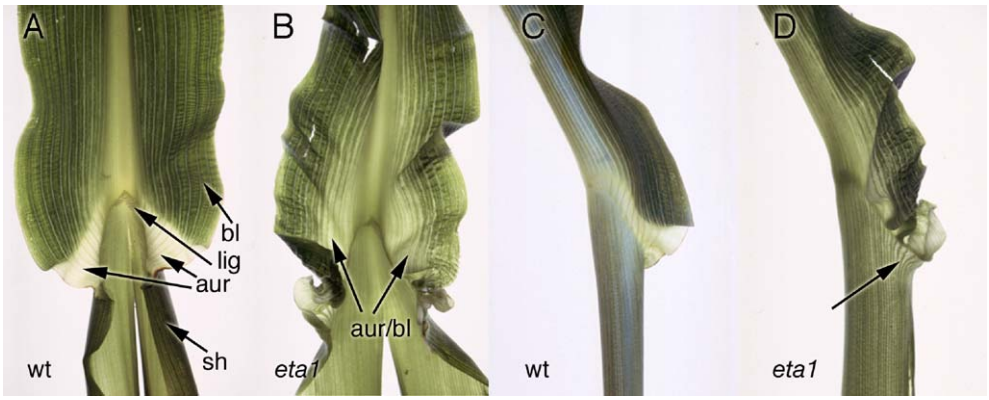

Fig. 1. Mature leaf phenotype of *eta1*. Leaf 11 of an *eta1-R* segregating family in the Mo17 background. (A) Adaxial view of a wild-type leaf at the blade/sheath boundary. (B) Adaxial view of an *eta1* leaf at the blade/sheath boundary, arrows point to diffuse auricle/blade boundary. (C) Abaxial side-view of a wild-type leaf. Notice the wedge-shaped auricle and discrete blade/sheath boundary. (D) Abaxial side-view of an *eta1* leaf. Notice the undulating auricle, displaced blade/sheath boundary and abnormal sheath venation (white arrow); bl = blade, lig = ligule, aur = auricle, and sh = sheath.

slightly reduced in B73, but not in W23 (Table 1). Sheath and blade width was not significantly affected in *eta1* mutants. This indicates that there is an overall reduction in leaf length, mainly in the sheath of *eta1* mutants, but leaf width is unaffected. When the sheath to blade length ratio is measured, the ratio is lower for *eta1* than wild type (Table 1). Therefore, the blade/sheath boundary is more proximal, or is basipetally displaced, in *eta1* mutants compared to wild type. Leaf development occurs basipetally in maize; this indicates that the blade/sheath boundary is formed earlier in wild type than in *eta1* mutants (Sylvester et al., 1990). These data are consistent with *eta1* affecting proximodistal regional identity in the leaf.

Vascular development and cellular organization are altered at the blade/sheath boundary in eta1 mutants

Correct vascular and cellular organization is required for proper leaf development. Therefore, we wanted to determine if vascular and cellular organization was perturbed in *eta1* mutant leaves. The maize leaf contains three types of longitudinal veins: the midvein, the lateral veins, and the intermediate veins. The midvein is first visible at p0–p1 (Sharman, 1942) and then lateral veins develop acropetally (from base to tip) during the primordial stage (Freeling and Lane, 1994). The smaller intermediate or basipetal veins branch from lateral veins initially, then develop basipetally (from tip to base), and anastamose (or coalesce) at the blade/sheath boundary (Russell and Evert, 1985; Sharman, 1942). To characterize the underlying vascular pattern in *eta1* mutants, vascular bundles were stained in leaves of individuals from an *eta1* segregating family. No differences in the midvein or the lateral veins were observed between wild-type and *eta1* mutant leaves (data not shown). However, while intermediate veins normally anastamose at the blade/sheath boundary in wild-type leaves, the intermediate veins anastamose over a wider range and can be found in the blade and sheath in *eta1* mutant leaves (Supplementary Fig. 1) Therefore, vascular development in *eta1* mutants occurs normally in the primordium when the midrib and lateral veins develop, but deviates from wild type during post-primordial intermediate vein development.

To determine the cellular organization of *eta1* mutant leaves, we examined transverse sections of blade, auricle, and sheath under UV auto-fluorescence. Wild-type and *eta1* seedling leaves were dissected and sectioned at transverse planes indicated in Figs. 2A and E (white lines). The number of intermediate veins in the proximal blade region just distal to the auricle is greatly reduced in *eta1* mutants compared to wild type (Figs. 2B versus F). In addition, there is accumulation of proto-lignins around the lateral veins of *eta1* blade, which is indicative of auricle regional identity (Figs. 2F, marked with asterisks, compare with wild-type blade, B; wild-type auricle, C; and *eta1* auricle, G). The cellular organization of the sheath is similar in wild type and *eta1* (Figs. 2D and H). These data show that *eta1* mutant defects are localized to the blade and auricle, confirm a mixed auricle/blade cell fate in *eta1* mutant blade, and further illustrate that the boundary between blade and auricle is diffuse and disorganized.

SEM analysis reveals that Eta1+ acts early in positioning of the blade/sheath boundary

Previous work has shown that *eta1* mutants fail to fully form a ligule fringe and show a displaced blade/sheath boundary. One explanation could be that auricle cells are simply enlarged. However, auricle cells are morphologically normal in size and shape, although somewhat disorganized (Osmont et al., 2003). We wanted to determine whether the blade/sheath boundary defect in *eta1* mutants was the result of aberrant establishment of the blade/sheath boundary or if only subsequent differentiation was perturbed. We examined early developing p9–p4 leaves in an *eta1* segregating family using Scanning Electron Microscopy. At p9, the ligule is mostly differentiated and appears normal over the midrib in both wild type and *eta1* mutants (Figs. 3A and B). However, in the marginal domain, the *eta1* mutant ligule fails to form completely, development is delayed, and organization is disrupted (Figs. 3C and D). In p8–p6 primordia, the ligule ridge divides and expands in an organized manner in wild type, but in *eta1* primordia the ligule ridge is disorganized (Figs. 3E, G, I and F, H, J). After the first synchronous anticlinal cell divisions, periclinal cell divisions commence around the p5 stage, and the preligule band is formed perpendicular to the proximodistal axis in wild type (Fig. 3K). In contrast, cell divisions in *eta1* primordia occur in a serpentine fashion across the adaxial leaf surface (Fig. 3L). The preligule band, which marks the first sign of blade/sheath boundary growth, is visible at p4 (Walsh et al., 1998). At p4, after the anticlinal divisions are initiated, cell divisions occur along a straight-line perpendicular to the proximodistal axis in wild type (Fig. 3M), whereas they occur at a curved angle in *eta1* mutants (Fig. 3N). Longitudinal and transverse divisions are observed in

Table 1
Affect of *eta1* on leaf dimensions

Background	*n*	Sheath length in cm (SD)	Sheath width in cm (SD)	Blade length in cm (SD)	Blade width in cm (SD)	Sheath to blade length ratio
B73						
wt	100	14.3 (±0.6)	3.9 (±0.8)	64.3 (±13.8)	4.5 (±1.0)	0.22
eta1	100	10.3 (±0.7)	4.1 (±0.8)	54.9 (±10.4)	4.7 (±1.2)	0.19
W23						
wt	100	17.3 (±1.1)	3.4 (±0.7)	51.7 (±14.1)	3.7 (±1.0)	0.33
eta1	100	11.7 (±0.5)	3.4 (±0.6)	48.8 (±12.1)	3.4 (±1.1)	0.24

All measurements were taken at the time of anthesis. Ten leaves were measured on 10 plants of each genotype.

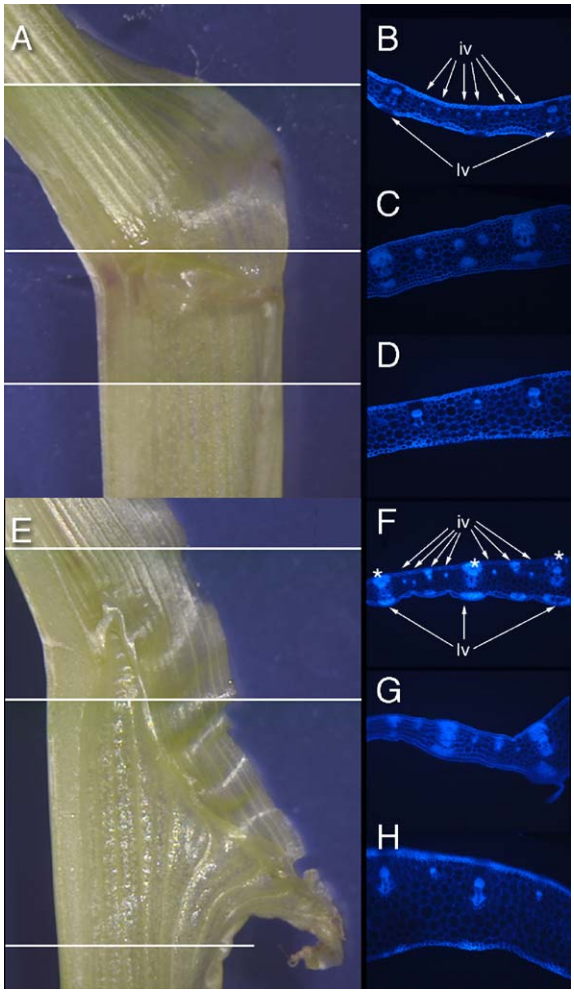

Fig. 2. (A–H) Transverse sections of seedling leaves of an *eta1* segregating family in the W23 background viewed with UV fluorescence. (A) Adaxial view of a wild-type leaf at the blade/sheath boundary. (E) Adaxial view of an *eta1* leaf at the blade/sheath boundary. Panels A and E are viewed at 6× under a dissecting microscope; white lines mark the planes of transverse sections. (B–D; F–H) Auto-fluorescence of lignin in transverse leaf sections at 50× magnification, abaxial surface is oriented to the top of the page and adaxial surface is oriented to the bottom of the page. (B) Wild-type blade; (C) wild-type auricle; (D) wild-type sheath; (F) *eta1*, blade; (G) *eta1* auricle; (H) *eta1* sheath. Designations in panels B and F mark intermediate veins (iv) and lateral veins (lv).

both wild type and *eta1* mutants (Figs. 3O and P). Thus, the plane of cell division at the blade/sheath boundary is not affected in *eta1* mutants; only the relative position of the cell divisions is altered.

Our SEM analysis shows that *Eta1+* acts during the establishment of the blade/sheath boundary because *eta1* defects are seen at the p4 stage concomitant with the first visible sign of the blade/sheath boundary. These results indicate that the *eta1* mutant fails to initiate the blade/sheath boundary in the correct position. In addition, these data show that the *eta1* mutant leaf phenotype is not solely due to differentiation defects, since auricle tissue differentiation occurs after initiation of the preligule band (Becraft et al., 1990). These data place *Eta1+* function at the positioning of the blade/sheath boundary, just when ligule and auricle begin to differentiate.

Mosaic analysis

Sector classes and their affect on leaf development

Mosaic analysis was performed to help elucidate the role of *Eta1+* in leaf development, and specifically in relation to development of the blade/sheath boundary. The experiment was designed to concurrently expose the recessive *eta1* mutant allele and a recessive, visible cell autonomous marker, *lw2*, conferring a chlorophyll deficiency (Hake and Freeling, 1986). *Eta1+Lw2+/eta1 lw2* individuals were X-irradiated resulting in sectors of white *eta1* tissue in a field of green wild-type tissue (Fig. 4).

A total of 111 sectors were obtained from 53 individuals. Only 20 passed through at least the blade/sheath boundary and showed an *eta1* phenotype (Table 2). Sector sizes ranged from 2 to 15 mm indicating that some sectors occurred later in development (2 mm) and others occurred earlier (15 mm). Leaves containing *eta1* mutant sectors showed a striking basipetal displacement of the blade/sheath boundary (Fig. 4B). The displacement phenotype ranged from 2 to 116 mm and was observed in 16/20 sectors (Table 2). Notably, the basipetal displacement of the blade/sheath boundary did not occur only in the *eta1* mutant sector but also occurred in the wild-type tissue between the sector and midrib. The four sectors that did not show displacement, either within or outside of the sector, did show disruption of the ligule and extension of auricle within the sector, as observed by light microscopy. Ligule disruption and auricle extension was only observed in the *eta1* mutant sectors, and not in the wild-type ligule and auricle tissue flanking those sectors. These four sectors were positioned near the midrib. These data indicate that the displacement phenotype is dependent on sector position along the mediolateral axis.

Contribution of tissue layer to eta1 phenotype

To determine the contribution of the different tissue layers to *eta1* phenotypes, sectors were divided based on the tissue layers contained in the *eta1 lw2* clonal sectors (Table 2 and Fig. 5). Class I was made up of eight sectors, in which all tissue layers were mutant for both *eta1* and *lw2* (Figs. 5A, B, and J). All Class I sectors showed a marked basipetal displacement of the blade/sheath boundary (Fig. 5A). Importantly, the wild-type tissue between the midrib and *eta1* sector also showed basipetal displacement. Thus, *eta1* mutant tissue, which presumably lacks *Eta1+* function, was able to displace wild-type tissue at the blade/sheath boundary.

Class II was comprised of seven sectors that were mutant for the adaxial epidermal and mesophyll layers (Figs. 5C, D, and K). Four of the seven sectors showed ligule disruption and auricle extension within the sector as well as basipetal displacement of the blade/sheath boundary in the wild-type tissue between the midrib and the sector. The other three sectors showed ligule disruption and auricle extension within the sector, but no displacement of the blade/sheath boundary outside of the sector. The difference between the phenotypes

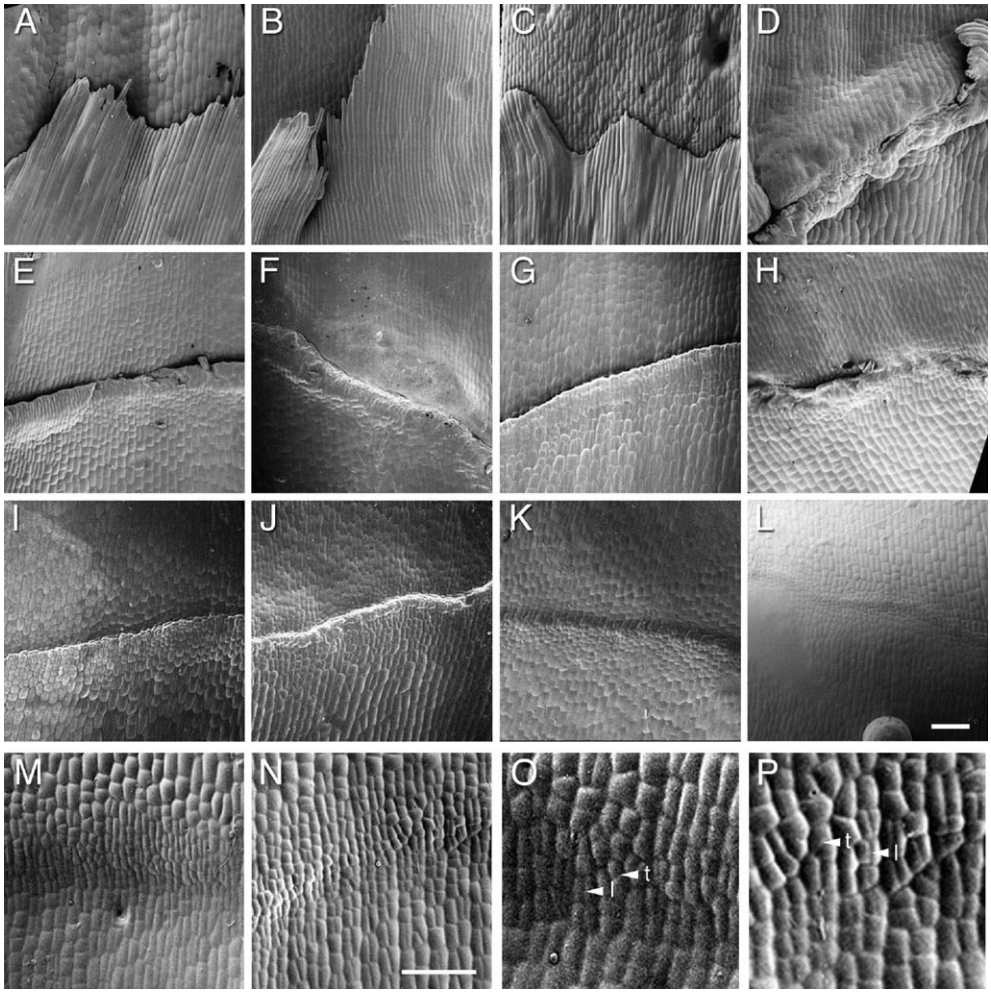

Fig. 3. SEM analysis of *eta1*. Adaxial view of developing leaves of an *eta1-R* segregating family in the W23 background at the blade/sheath boundary. (A) Wild-type L6, p9 just flanking midrib; (B) *eta1* L6, p9 just flanking midrib; (C) wild-type L6, p9 at the margin; (D) *eta1* L6, p9 at the margin; (E) wild-type L7, p8 at the late ligule ridge stage; (F) *eta1* L7, p8 at the late ligule ridge stage; (G) wild-type L8, p7 at the ligule ridge stage; (H) *eta1* L8, p7 at the ligule ridge stage; (I) wild-type L9, p6 at the ligule ridge stage; (J) *eta1* L9, p6 at the ligule ridge stage; (K) wild-type L10, p5 at the pre-ligule band stage; (L) *eta1* L10, p5 at the pre-ligule band stage, scale bar = 100 μm; (M) wild-type L11, p4 anticlinal division at the pre-ligule band stage; (N) *eta1* L11, p4 anticlinal division at the pre-ligule band stage; (O) wild-type L11, p4; (P) *eta1* L11, p4, arrowheads point to (t) transverse and (l) longitudinal cell divisions, scale bar = 100 μm.

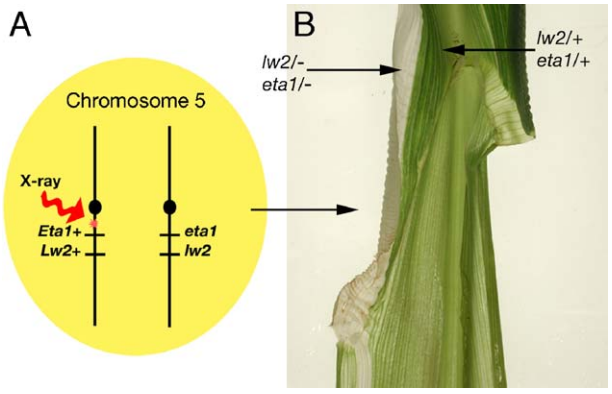

Fig. 4. Mosaic analysis of *eta1*. (A) Imbibed kernels were irradiated with X-rays, which a small fraction of the time caused the breakage of one of the long arms of Chromosome 5 carrying the wild-type *Lw2+* and *Eta1+* alleles. When this arm is broken, a sector of white *lw2 eta1* tissue is uncovered. (B) Abaxial view of a sector showing *eta1* phenotype in a *eta1 lw2* clonal sector.

displayed correlated with lateral sector position on the leaf. Mainly, the sectors near the midrib did not show displacement, while more marginal sectors did show displacement. These data suggest that the medial and lateral leaf domains may have a different requirement for *Eta1+*.

Class III consisted of three sectors that were mutant for the internal mesophyll layers. Both the adaxial and abaxial epidermal layers were wild type (Figs. 5E, F, and L). All three internal sectors displayed ligule disruption and auricle extension within the sector and showed displacement of the blade/sheath boundary in the wild-type tissue between the midrib and proximal sector boundary. This sector class is informative because it shows that wild-type epidermal layers are not sufficient to prevent either basipetal displacement or the disrupted ligule and auricle extension phenotypes.

Class IV contained two sectors each with a combination of mutant epidermal and mesophyll layers (Figs. 5G, H, M, and N). Both sectors showed ligule disruption and auricle extension

Table 2
Mosaic sector analysis

Sector class	Sector description				
	Leaf number	Sector width (mm)	Displacement (mm)	Lateral position	Sector range
I. All tissue layers mutant (8)	L4	8	71	l	0.65–1
	L6	15	92	l	0.7–1
	L16	6	20	l	0.71–1
	L8	8	75	l	0.68–1
	L4	1	11	ml	0.45–0.5
	L9	11	100	ml	0.49–0.73
	L9	5	15	m	0.26–0.33
	L10	1	10	m	0.25–0.27
II. One epidermal and one mesophyll layer mutant (7)	L7	13[a]	116	l	0.71–1
	L10	9[a]	22	l	0.81–1
	L6	10[a]	22	l	0.81–1
	L8	5[a]	None	m	0.21–0.39
	L6	12	None	m	0.27–0.52
	L12	3	19	m	0.27–0.32
	L11	1	None	m	0.18–0.64
III. All internal mesophyll layers mutant (3)	L9	5	2	l	0.87–0.98
	L7	11	64	l	0.78–1
	L9	9	34	l	0.67–0.84
IV. Two internal mesophyll layers mutant (2)	L4	2	15	l	0.78–0.87
	L2	1	None	ml	0.5–0.66

[a] Approximate measurements based on microscopy due to poorly visible sector boundaries; l = lateral (marginal half of the leaf), ml = midway between midrib and margin, m = medial (midrib half of the leaf).

within the sector. One sector showed basipetal displacement of the blade/sheath boundary, while the other sector, near the midrib, did not.

When all internal mesophyll layers were mutant (Classes I and III), basipetal displacement of the blade/sheath boundary in the wild-type tissue between the midrib and the sector boundary was always observed. When one or more mesophyll layer was wild type (Classes II and IV), marginal sectors showed basipetal displacement of the blade/sheath boundary, while sectors near the midrib did not. Therefore, if *Eta1+* is lost in all internal mesophyll layers, displacement of the blade/sheath boundary is observed, regardless of the mediolateral sector position on the leaf. However, if *Eta1+* function remains in at least one internal mesophyll cell layer and the sector is near the midrib, displacement does not occur, but the ligule is still disrupted and auricle still extends into blade. These data indicate that there is a differential response to loss of wild-type *Eta1+* function along the mediolateral axis of the leaf.

The basipetal blade/sheath boundary displacement phenotype is independent of sector width

The severity of *eta1* phenotype and basipetal displacement does not correlate with sector width (Fig. 6). For example, a narrow sector can show a large amount of basipetal displacement (Fig. 6A), while a wide sector can show a small amount of basipetal displacement (Fig. 6B). While many of the sectors were at or near the margin (Fig. 6G), the sectors in the middle of the leaf were informative as they had wild-type tissue on either side (Figs. 6B–F). In all cases, auricle tissue was continuous from the midrib to the margin and did not reinitiate on the marginal side of the sector. These data indicate that, although the *eta1* sector displaces the blade/sheath boundary, the ligule and auricles form continuously. Moreover, cells on the marginal side of the sector are still competent to respond to the developmental signals to form ligule and auricle. Thus, the *eta1* sector still conveys positional and developmental information to the wild-type tissue flanking the sector.

Discussion

Our data indicate that *Eta1+* is required for proper positioning and differentiation of the blade/sheath boundary. The most obvious morphological defect of *eta1* mutant leaves is an extension of proximal auricle tissue into distal blade (Fig. 1), implicating a role for *eta1* in proximodistal patterning of the maize leaf. Based on our measurements of leaf dimensions (Table 1), the position of the blade/sheath boundary is basipetally displaced in *eta1* mutants. Since post-primordial leaf differentiation progresses from leaf tip to base, these data suggest that the differentiation of the blade/sheath boundary is delayed in *eta1* mutants. In addition, we reveal that *eta1* is required for proper vascular and cellular differentiation at the blade/sheath boundary (Fig. 2). Because SEM and mosaic analyses showed that the *eta1* phenotype becomes progressively more severe as the blade/sheath boundary extends laterally, these data implicate a role for *Eta1+* in mediolateral signaling (Figs. 3, 5, and 6). In addition, these data indicate an increased requirement for *Eta1+* function from the midrib to the margin of the leaf.

Mutant eta1 sectors affect the development of the blade/sheath boundary in wild-type tissue

The most striking phenotype of *eta1* mosaic leaves is the basipetal displacement of the blade/sheath boundary. This

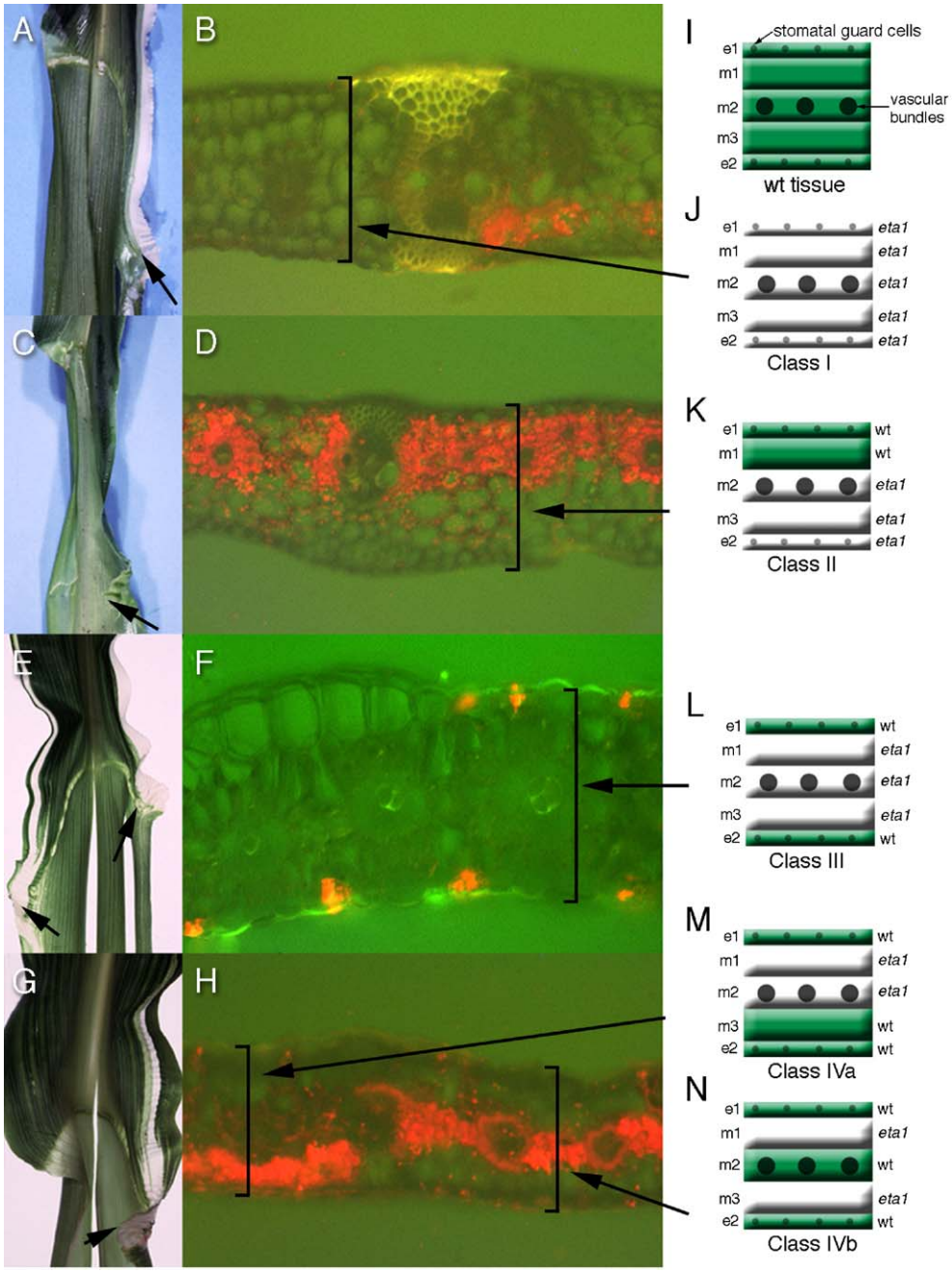

Fig. 5. Representative sectors of the four sector classes. (A, C, E, G) Ad/abaxial views of the leaf containing the sector, illustrating the basipetal displacement of the blade/sheath boundary when an *eta1* sector is present. (B, D, F, H) Transverse sections of the leaves in panels A, C, E, and G in the region of the sector, adaxial surface is oriented towards the top of the page. (A) Adaxial view of a Class I sector. (B) All layers lack the *lw2* marker linked to *eta1* therefore no chlorophyll fluorescence is observed. (C) Adaxial view of a Class II sector. (D) Abaxial epidermis and mesophyll layers mutant. (E) Abaxial view of a Class III sector. (F) All internal mesophyll layers mutant, only both epidermal layers contain chlorophyll. (G) Adaxial view of a Class IV sector. (H) Partial internal mesophyll layers mutant. (I–N) Cartoon representations of transverse leaf sections defining sector classes. (I) Wild-type tissue, no sector. (J) Sector Class I all layer mutant for *eta1* and the *lw2* marker (no red chlorophyll auto fluorescence). (K) Sector Class II. (L) Sector Class III. (M) Sector Class IV a. (N) Sector Class IV b. e1 = adaxial epidermis, m1 = adaxial mesophyll, m2 = middle mesophyll, m3 = abaxial mesophyll, e2 = abaxial epidermis.

displacement correlates with the sector position along the mediolateral axis of the leaf. The more lateral the sector, the more the blade/sheath boundary is basipetally displaced. However, in *eta1* sectors, the timing (width) of the sector does not correlate with the phenotype or severity of basipetal displacement. In contrast, mosaic analysis with *Lg3* showed that the timing of sector initiation determined regional fate of the sector (Muehlbauer et al., 1997). Essentially, the earlier the wild-type *lg3+* sector is induced during development (the larger the sector), the more proximal the regional fate is. These data indicate that *Eta1+* function is likely required throughout the leaf maturation process. Alternatively, the displacement phenotype could simply be a biophysical outcome of *eta1* delaying the development of the blade/sheath boundary, similar

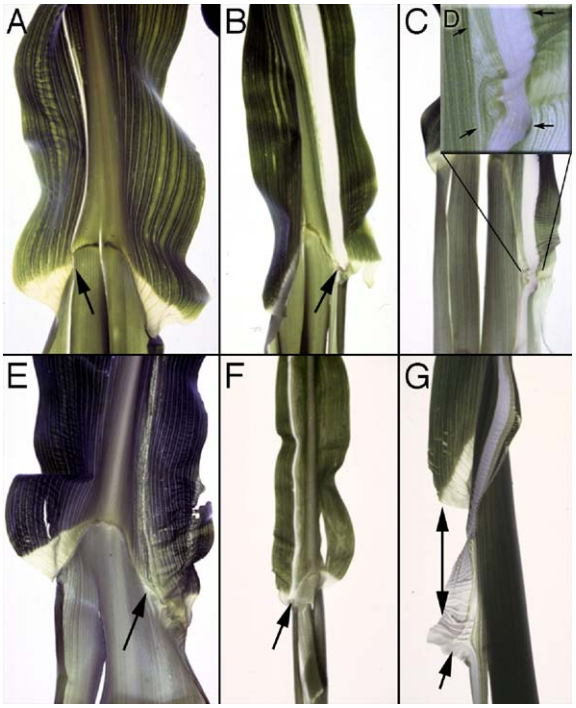

Fig. 6. Informative *eta1 lw2* sectors. (A) Adaxial view of a narrow sector with basipetal displacement (arrow). (B) Adaxial view of a wider sector with small basipetal displacement. (C) Abaxial view of sector with wild-type ligule and auricle flanking the sector. (D) Close-up of the blade/sheath boundary in the sector, black arrows mark the boundaries of the sector. (E) Adaxial view of a narrow sector. (F) Adaxial view of a wide sector. (G) Adaxial view of a marginal sector, arrow points to the basipetal displacement of the blade/sheath boundary.

to the stress-induced differential growth observed in *D8* mosaic sectors (Harberd and Freeling, 1989).

A surprising finding is that *eta1*, a recessive allele and presumably a loss-of-function allele, can affect the surrounding wild-type tissue. This phenomenon has been previously documented in *Drosophila*, when marked *fz* mitotic clones are induced in the *Drosophila* wing (Vinson and Adler, 1987). Essentially, wild-type cells located distally to the *fz* clonal sector produce hairs that are oriented towards the mutant sector (Adler and Lee, 2001). *fz* is part of the *Wnt* signalling pathway, which plays various roles in *Drosophila* development. Thus far, a few homologs of the *Wnt* signaling pathway have been identified in plants and have been implicated in hormone signaling (Amador et al., 2001; Li and Nam, 2002).

The contribution of tissue layer to the eta1 phenotype

Mosaic analyses in maize have established the importance of cell-to-cell communication at the boundaries of the tissue layers in the transverse (adaxial–abaxial) dimension of the leaf. For example, mutant mesophyll layers induced epidermal knots on wild-type epidermis in dominant *Kn1* mosaic leaves (Hake and Freeling, 1986), and mosaic analyses of both the *Gn1* and *Wab1* dominant mutants showed cell autonomy in the lateral dimension and non-cell autonomy in the transverse dimension (Foster et al., 1999a, 2004). The ligule disruption and auricle extension phenotypes were seen in all *eta1* sectors regardless of the displacement phenotype or tissue layer affected, which indicates that *Eta1+* is required transversely in all internal mesophyll layers for proper positioning and differentiation of ligule and auricle, as even only one internal mutant tissue layer can cause the *eta1* phenotype within the sector. One explanation is that proper formation of the blade/sheath boundary requires the coordination and communication of all cell layers, perhaps via a secondary signal that is received or mediated by *Eta1+*. Clearly, wild-type *Eta1+* in adjacent tissue layer cannot rescue the *eta1* mutant sectors because a wild-type phenotype in the sector would be expected, not an *eta1* phenotype as we observe. These data indicate *Eta1+* function is required in all of cell layers of the transverse dimension of the leaf because even wild-type mesophyll layers cannot rescue the *eta1* mutant phenotype.

A two-way signaling pathway for blade/sheath boundary formation

As observed with *eta1* sectors, mosaic analysis of a specific *lg1* sector class, in which all tissue layers were mutant, resulted in basipetal displacement of the blade/sheath boundary 40% of the time (Becraft and Freeling, 1991) (Fig. 7). These workers observed that ligule and auricle tissue reinitiated in a more basipetal position on the marginal side of *lg1* sectors. However, in *eta1* sectors, the basipetal displacement occurs in sectors regardless of which tissue layers are mutant (Fig. 5). In addition, *eta1* sectors show a continuation of ligule and auricle development and not a reinitiating of ligule and auricle as in *lg1* sectors (Becraft and Freeling, 1991) (Figs. 6 and 7). An important difference between *lg1* and *eta1* sectors is that *eta1* mutant sectors affect wild-type tissue flanking the sector. This

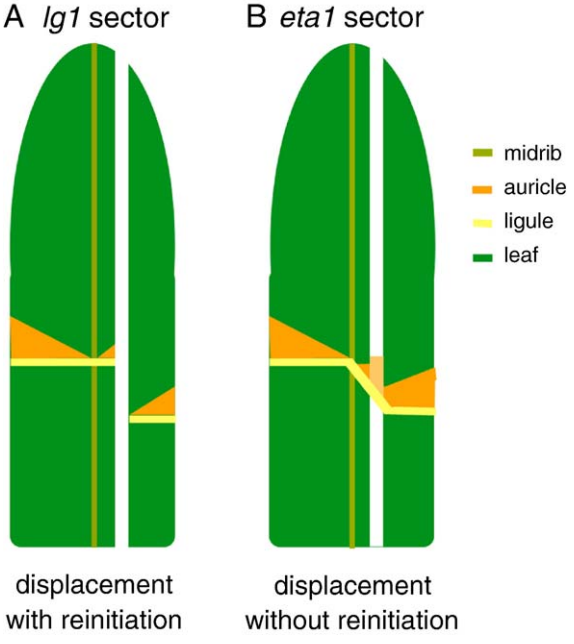

Fig. 7. A schematic depicting *lg1* and *eta1* sectors. (A) In wild-type tissue flanking *lg1* sectors, there is "reinitiation" of the ligule and auricle. (B) In wild-type tissue flanking *eta1* sectors, there is no "reinitiation" and ligule and auricle are continuous.

indicates that there must be cell-to-cell communication between the wild-type and *eta1* mutant tissue. In *eta1* sectors, the *Lg1+* signal is still presumably present and, therefore *eta1* mutant tissue is still competent to respond to the signal to form ligule and auricles.

Sectors of *eta1* mutant tissue retard the development of the blade/sheath boundary even in wild-type tissue. If *Eta1+* functions only in positioning the blade/sheath boundary, the expectation would be that displacement would only be seen in the sector, and not, as we observe, in wild-type tissue outside the sector. *Eta1+* and *Lg1+* may function in similar contexts because mutant sectors of both in wild-type leaves cause basipetal displacement of the blade/sheath boundary (Fig. 7). In addition, *eta1* and *lg1* interact synergistically based on double-mutant analysis (Osmont et al., 2003). Furthermore, *lg1* and *Kn1* sectors provide evidence for a "make-ligule/auricle" signal that begins near the midrib and proceeds in two foci towards the leaf margins (Becraft and Freeling, 1991; Hake and Freeling, 1986; Sylvester et al., 1990). Previous work has shown that differentiation occurs basipetally in maize leaves (Sylvester et al., 1990). In *lg2* mutant leaves, the blade/sheath boundary fails to initiate near the midrib, but recovers in the lateral dimension (Walsh et al., 1998), and the blade/sheath boundary in *lg2* mutants is often displaced, occurring at different points along the proximodistal axis on opposite sides of the same leaf (Harper and Freeling, 1996). This indicates that there is a range of competency along the proximodistal axis for ligule and auricle initiation and differentiation.

Because the blade/sheath boundary is continuous in *eta1* sectors, we suggest that there is a two-way signaling from the margin back to the midrib. That is, the presence of an *eta1* mutant sector influences the development of the rest of the leaf, as even wild-type tissue is displaced between the midrib and *eta1* sector.

The *eta1* mosaic results suggest that *Eta1+* functions somewhere in the response to signals involving position-dependent differentiation. The continuity seen with *eta1* sectors implies that there must be a mandate for the ligule to remain continuous even when displaced and suggests a previously unnoticed level of signaling. Double-mutant analysis of *eta1* and *lg2* shows a dominant dosage effect (Osmont et al., 2003). Homozygous *lg2* plants that are heterozygous for *eta1* show extension of auricle into blade, a phenotype not observed in plants heterozygous for *eta1* or single *lg2* mutants. This genetic interaction between *lg2* and *eta1* suggests both genes are required for the proper positioning of the blade/sheath boundary and that LG2 could be the signal responsible for repositioning the blade/sheath boundary in wild-type tissue flanking *eta1* sectors. The mosaic analysis conducted with *lg2* is consistent with this, since sectors of *lg2* mutant tissue are rescued by adjacent wild-type tissue (Harper and Freeling, 1996). Therefore, the phenotype of *eta1* mosaic leaves could be due to LG2 function, which is thought to act in the transition from blade to sheath (Walsh and Freeling, 1999; Walsh et al., 1998). These data indicate that there is a feedback mechanism involved in patterning the blade/sheath boundary and that *Eta1+* is involved in this signaling pathway. The *Rld1* mutant provides a precedent for this type of feedback mechanism in adaxial–abaxial patterning of the leaf (Nelson et al., 2002).

A model for Eta1+ function in the maize leaf

Based on our analyses, *Eta1+* function may be modeled. First, SEM analysis of *eta1* leaf primordia has shown that the *Eta1+* gene functions early in the placement of the blade/sheath boundary (but after primordial development and lateral vein initiation), as the pattern of cell division is altered as early as the p4 stage of leaf development. In addition, the severity of the *eta1* mutant phenotype increases from the midrib to the margin. Second, *eta1* mutants interact genetically with mutants of both *Knox* and *lg* genes, showing enhancement and dominant dosage interactions (Osmont et al., 2003). Since *eta1* leaves do not ectopically express *KNOX* genes or alter *LG1* or *LG2* expression, the *eta1* mutant phenotype cannot be

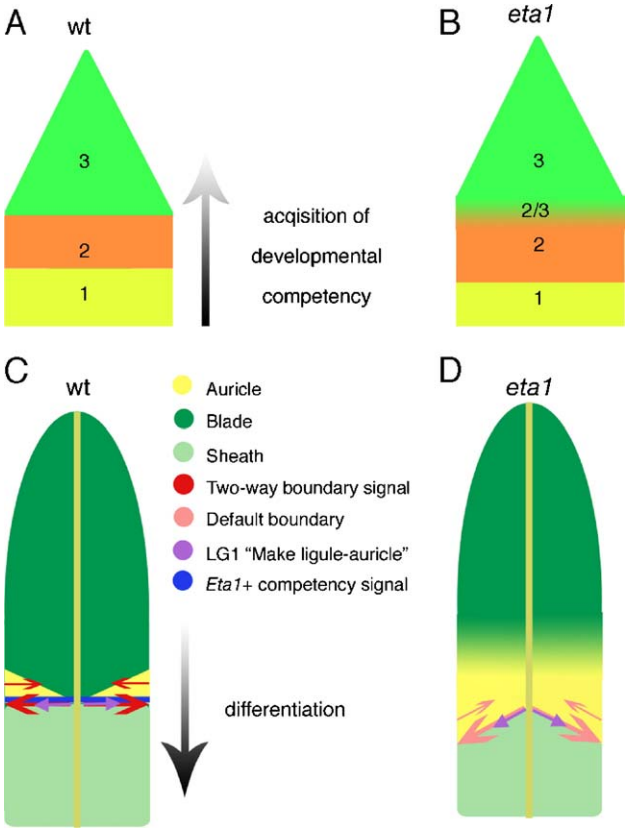

Fig. 8. *Eta1+* functions both in acquisition of developmental competencies and in differentiation of the blade/sheath boundary. (A) The maturation schedule hypothesis states that a wild-type leaf primordium acquires developmental competencies in an acropetal wave from base to tip. 1 = sheath competency, 2 = auricle/ligule competency, 3 = blade competency. (B) *eta1* mutant leaf primordia undergo a precocious transition from sheath (1) to ligule/auricle (2) and the blade sheath boundary is a mosaic of 2/3 auricle/blade competencies. (C) During differentiation, *Eta1+* functions to promote competency from midrib to the margin, which aids in positioning the blade/sheath boundary, likely with the help of LG2 and perhaps other unknown non-cell autonomous factors (red arrows). Once the boundary is laid down, the "make ligule-auricle" signal encoded by LG1 is propagated (purple arrows). (D) In *eta1* mutants, the *Eta1+* competency signal is absent. The blade/sheath boundary forms along a default boundary in a more basipetal position, and the two-way blade/sheath boundary-positioning signal is delayed (pink arrows).

explained by aberrant transcriptional regulation of these genes. Since *eta1* enhances *Knox* mutant phenotypes, the increased sensitivity to ectopic *KNOX* expression in the double mutant individuals could be caused by an increase in competency to respond to the ectopic KNOX signal in the absence of *Eta1+*. Third, mosaic analysis reveals that wild-type *Eta1+* tissue cannot rescue *eta1* mutant tissue, and that *Eta1+* acts with other factors, presumably LG2, during the positioning of the blade/sheath boundary.

Based on these three conclusions, we propose a model whereby *ETA1* functions both in acquisition of developmental competencies (Figs. 8A and B) and in differentiation of the blade/sheath boundary (Figs. 8C and D). The maturation schedule hypothesis states that all cells within a p1–p3 leaf primordium progress through the same stages of potential identity (sheath to auricle to blade), but different regions (e.g. Proximal) go through these competency stages at different times (Freeling, 1992; Muehlbauer et al., 1997). Just prior to differentiation, the leaf primordium is made up of sheath, ligule/auricle, or blade competencies along the proximodistal axis (Fig. 8A). In *eta1* mutant primordia, cell fate is altered by perturbations in the maturation schedule, and ligule/auricle competencies are both precocious and intermixed with blade competency (Fig. 8B). Therefore, *Eta1+* could be a universal part of the system that maintains regional identity. *Eta1+* function could define competency by mediating the response to a particular set of gene activities, perhaps via changes in chromatin state. Notably, *mop1*, a mutant that affects epigenetic phenomena (Dorweiler et al., 2000), partially suppresses the *eta1* phenotype in the leaves (K.S.O. and M.F., unpublished data). A downstream consequence of ectopic *KNOX* gene expression in leaves, which retards the maturation schedule (Muehlbauer et al., 1997), is likely to down-regulate *Eta1+*. This might mean that auricle regional identity may be ambiguous. Thus, all signals passing through "auricle" cells will pass more slowly, extant differentiation proceeds unimpeded, and identities that should be locked-in are now still open for additional, ambiguous signaling.

Various regions in the leaf primordium express their acquired regional identity by differentiating into sheath ligule/auricle or blade based on their potential (competence) at the time when the differentiation signal arrives. In wild-type primordium, *Eta1+* functions to promote competency to respond to other gene activities essential to form the blade/sheath boundary, mainly LG2 and LG1 (Fig. 8C). In *eta1* mutants, the shape of the ligule line is altered by changes in regional identity, but also by changes that end up altering mediolateral communication pathways, as deduced from mosaic experiments. Thus, when *Eta1+* function is lost, this region becomes hypersensitive to perturbations in the signaling and development of the blade/sheath boundary, as evidenced by the severe double mutant phenotypes and dosage effects with *Knox* and *lg* mutants (Osmont et al., 2003). In the *eta1* single mutant, the blade/sheath boundary still forms. This could be explained by the range of competency along the proximodistal axis, suggested by *lg1* and *lg2* genetic analyses and the proposed presence of a default blade/sheath boundary (Fig. 8D) (Becraft and Freeling, 1991; Becraft et al., 1990; Harper and Freeling, 1996).

We demonstrate that *eta1* is a novel and integral regulator of maize post-primordial leaf development that acts both early in the positioning of the blade/sheath boundary and later in differentiation of the ligule and auricles. We also show that *eta1* functions autonomously in the mediolateral axis of the leaf, and provide evidence for a non-autonomous two-way signaling pathway involved in blade/sheath boundary formation.

Acknowledgments

We would like to thank Bjorn Rydberg and the Cooper Lab at Lawrence Berkeley National Labs for training and use of their X-ray machine; Steve Ruzin and Denise Schichnes at the UC-Berkeley CNR Biological Imaging Facility for the use of their microscopes and their technical assistance; the Electron Microscope Lab at UC-Berkeley for assistance with SEM analysis; and to members of the Freeling lab, Jennifer Fletcher, George Chuck, Lynne Jesaitis, and Sheila McCormick for critical reading and comments on the manuscript. This work was supported by the National Institutes of Health grant 5R01 GM42610 to M.F and the Haas Scholars Fellowship from UC-Berkeley to N.S.

Appendix A. Supplementary data

Supplementary data associated with this article can be found, in the online version, at doi:10.1016/j.ydbio.2005.11.012.

References

Adler, P.N., Lee, H., 2001. *Frizzled* signaling and cell–cell interactions in planar polarity. Curr. Opin. Cell Biol. 13, 635–640.

Amador, V., Monte, E., Garcia-Martinez, J.L., Prat, S., 2001. Gibberellins signal nuclear import of PHOR1, a photoperiod-responsive protein with homology to *Drosophila* armadillo. Cell 106, 343–354.

Becraft, P., Freeling, M., 1991. Sectors of *liguleless*-1 tissue interrupt an inductive signal during maize leaf development. Plant Cell 3, 801–808.

Becraft, P.W., Freeling, M., 1994. Genetic analysis of *rough sheath1* developmental mutants of maize. Genetics 136, 295–311.

Becraft, P.W., Bongard-Pierce, D.K., Sylvester, A.W., Poethig, R.S., Freeling, M., 1990. The *liguleless*-1 gene acts tissue specifically in maize leaf development. Dev. Biol. 141, 220–232.

Brink, R.A., 1933. Heritable characters in maize XLV1-*liguleless2*. J. Hered. 24, 325–326.

Dorweiler, J.E., Carey, C.C., Kubo, K.M., Hollick, J.B., Kermicle, J.L., Chandler, V.L., 2000. *Mediator of paramutation*1 is required for establishment and maintenance of paramutation at multiple maize loci. Plant Cell 12, 2101–2118.

Emerson, R.A., 1912. The inheritance of the ligule and auricles of corn leaves. Annu. Rep.-Nebr. Agric. Exp. Stn. 25, 81–88.

Foster, T., Veit, B., Hake, S., 1999a. Mosaic analysis of the dominant mutant, *Gnarley1-R*, reveals distinct lateral and transverse signaling pathways during maize leaf development. Development (Cambridge) 126, 305–313.

Foster, T., Yamaguchi, J., Wong, B.C., Veit, B., Hake, S., 1999b. *Gnarley1* is a dominant mutation in the *knox4* homeobox gene affecting cell shape and identity. Plant Cell 11, 1239–1252.

Foster, T., Hay, A., Johnston, R., Hake, S., 2004. The establishment of axial patterning in the maize leaf. Development 131, 3921–3929.

Fowler, J.E., Freeling, M., 1996. Genetic analysis of mutations that alter cell fates in maize leaves: dominant *liguleless* mutations. Dev. Genet. 18, 198–222.

Freeling, M., 1992. A conceptual framework for maize leaf development. Dev. Biol. 153, 44–58.

Freeling, M., Lane, B., 1994. The maize leaf. In: Freeling, M., Walbot, V. (Eds.), "The Maize Handbook", pp. 17–28. Springer-Verlag New York, Inc., 175 Fifth Avenue, New York, New York 10010, USA, Springer-Verlag, Heidelberger Platz 3, D-1000 Berlin, Germany.

Hake, S., Freeling, M., 1986. Analysis of genetic mosaics shows that the extra epidermal cell divisions in Knotted mutant maize plants are induced by adjacent mesophyll cells. Nature (London) 320, 621–623.

Harberd, N., Freeling, M., 1989. Genetics of dominant gibberellin-insensitive dwarfism in maize. Genetics 121, 827–838.

Harper, L., Freeling, M., 1996. Interactions of *liguleless1* and *liguleless2* function during ligule induction in maize. Genetics 144, 1871–1882.

Hay, A., Barkoulas, M., Tsiantis, M., 2004. *PIN*ning down the connections: transcription factors and hormones in leaf morphogenesis. Curr. Opin. Plant Biol. 7, 575–581.

Li, J., Nam, K.H., 2002. Regulation of brassinosteroid signaling by a GSK3/SHAGGY-like kinase. Science 295, 1299–1301.

Moreno, M.A., Harper, L.C., Krueger, R.W., Dellaporta, S.L., Freeling, M., 1997. *Liguleless1* encodes a nuclear-localized protein required for induction of ligules and auricles during maize leaf organogenesis. Genes Dev. 11, 616–628.

Muehlbauer, G.J., Fowler, J.E., Freeling, M., 1997. Sectors expressing the homeobox gene *liguleless3* implicate a time-dependent mechanism for cell fate acquisition along the proximal–distal axis of the maize leaf. Development (Cambridge) 124, 5097–5106.

Nelson, J.M., Lane, B., Freeling, M., 2002. Expression of a mutant maize gene in the ventral leaf epidermis is sufficient to signal a switch of the leaf's dorsoventral axis. Development 129, 4581–4589.

Osmont, K.S., Jesaitis, L.A., Freeling, M., 2003. The *extended auricle1 (eta1)* gene is essential for the genetic network controlling post-initiation maize leaf development. Genetics 165, 1507–1519.

Poethig, S., 1989. Genetic mosaics and cell lineage analysis in plants. Trends Genet. 5, 273–277.

Russell, S.H., Evert, R.F., 1985. Leaf vasculature in *Zea mays*. Planta (Heidelberg) 164, 448–458.

Sharman, B., 1942. Developmental anatomy of the shoot of *Zea mays* L. Ann. Bot. 6, 245–284.

Smith, L.G., Greene, B., Veit, B., Hake, S., 1992. A dominant mutation in the maize homeobox gene, *Knotted-1*, causes its ectopic expression in leaf cells with altered fates. Development (Cambridge) 116, 21–30.

Sylvester, A.W., Cande, W.Z., Freeling, M., 1990. Division and differentiation during normal and *liguleless-1* maize leaf development. Development (Cambridge) 110, 985–1000.

Theodoris, G., Inada, N., Freeling, M., 2003. Conservation and molecular dissection of *ROUGH SHEATH2* and *ASYMMETRIC LEAVES1* function in leaf development. Proc. Natl. Acad. Sci. U. S. A. 100, 6837–6842.

Tsiantis, M., Hay, A., 2003. Comparative plant development: the time of the leaf? Nat. Rev., Genet. 4, 169–180.

Vinson, C.R., Adler, P.N., 1987. Directional non-cell autonomy and the transmission of polarity information by the *frizzled* gene of *Drosophila*. Nature 329, 549–551.

Vollbrecht, E., Veit, B., Sinha, N., Hake, S., 1991. The developmental gene *Knotted-1* is a member of a maize homeobox gene family. Nature (London) 350, 241–243.

Walsh, J., Freeling, M., 1999. The *liguleless2* gene of maize functions during the transition from the vegetative to the reproductive shoot apex. Plant J. 19, 489–495.

Walsh, J., Waters, C.A., Freeling, M., 1998. The maize gene *liguleless 2* encodes a basic leucine zipper protein involved in the establishment of the leaf blade-sheath boundary. Genes Dev. 12, 208–218.